

RESEARCH

Open Access



# Development and validation of optimized lentivirus-like particles for gene editing tool delivery with Gag-Only strategy

Jinlin Jia<sup>1,2,3†</sup>, Yanzhe Hao<sup>4\*†</sup>, Lu Zhang<sup>1,2,3</sup>, Xiaofang Cao<sup>1,2,3</sup>, Lisha An<sup>1,2,3</sup>, Hu Wang<sup>1,2,3</sup>, Qi Ma<sup>4</sup>, Xiaohua Jin<sup>1,2,3\*</sup> and Xu Ma<sup>1,2,3\*</sup>

## Abstract

**Background** The development of gene editing tools such as CRISPR-Cas9 and base editors (BE) is critical for genetic diseases and cancer. Lentivirus-like particles (LVLPs) grows into an auspicious platform for delivering mRNA or ribonucleic proteins (RNPs) due to it integrates the advantage of viral and non-viral vectors. Current LVLP systems predominantly utilize HIV-Gag and Pol proteins. However, the reverse transcriptase and integrase of Pol, pose risks of genomic integration and potential tumorigenesis. Enhancing the safety of VLP system is essential. This study focuses on improving the LVLP to minimize these risks.

**Methods** We implemented a Gag-Only strategy, constructing LVLPs with HIV-Gag protein, thereby eliminating the integration risks linked to Pol. By leveraging the interactions between MS2-MCP (MS2 coat protein), PP7 and PP7 BP (PP7 binding protein), and the psi (HIV packaging signal) with HIV-Gag, we encapsulated PAMless andesine base editor (CE-8e-SpRY) mRNA and sgRNA targeting the PD1 start codon (ATG) into the LVLP. Using recombinant lentiviral vector technology, we developed a stable PD1-expressing 293T cell line (PD1-293T) to assess the editing efficiency of LVLP.

**Results** The psi-LVLP demonstrated effective packaging capabilities, achieving 15% base editing efficiency in 293T cells. By optimizing plasmid ratios, we observed increased CE-8e-SpRY mRNA copy numbers, with 30% base editing efficiency. Additionally, the integration of HDVrz (hepatitis delta virus ribozyme) and psi into sgRNA (HDVrz-psi-LVLP) substantially enhanced sgRNA copy numbers, resulting in approximately 50% base editing efficiency in 293T cells and 20% base editing efficiency in Jurkat cells. Mendelian randomization analyses revealed significant genetic correlations between PD1, B2M, CIITA, and TIGIT genes with various cancer risks. Furthermore, HDVrz-psi-LVLPs targeting the start codons of B2M, CIITA, and TIGIT exhibited high base editing activity in both Jurkat and 293T cells.

**Conclusion** In conclusion, this optimized platform effectively encapsulates CE-8e-SpRY mRNA and sgRNA, achieving high editing efficiencies across multiple genes and cell types. We introduce a safer and more efficient gene editing

<sup>†</sup>Jinlin Jia and Yanzhe Hao have contributed equally.

\*Correspondence:

Yanzhe Hao

haoyz@ivdc.chinacdc.cn

Xiaohua Jin

jinxiaohua96@163.com

Xu Ma

maxu\_fg@nrifp.org.cn

Full list of author information is available at the end of the article



tool delivery system by constructing LVLPs based on the Gag-Only strategy. Our study presents a promising implication for cancer immunotherapy.

**Keywords** Lentivirus-like particles (LVLPs), mRNA, Base editing, Packaging signal, Gag-only

## Introduction

Gene editing technologies such as CRISPR-Cas9, herald a transformative era in the precision genomic modification of living organisms [1, 2]. These methodologies not only promise to rectify the genetic underpinnings of myriad diseases, but also introduce challenges that necessitate rigorous comprehensive inquiry and innovation. CRISPR-Cas9 has revolutionized potential to edit genomes with precision. However, the technique often requires the induction of double-stranded DNA breaks (DSBs), which can lead to unintended genomic alterations such as insertions, deletions, and complex rearrangements [3, 4]. In contrast, base editing (BE), which includes cytosine base editors (CBEs) and adenine base editors (ABEs), facilitates targeted single-nucleotide conversions without inducing DSBs, thus significantly mitigating these adverse effects [5]. These cutting-edge base editing agents have been employed to successfully ameliorate disease associated-phenotypes by correcting pathogenic mutations across several types of cells, including human and nonhuman primates [6, 7], underscoring the potential of base editing as a therapeutic avenue.

Despite these promising outcomes, the widespread application of base editing is contingent upon the development of safe and effective delivery mechanisms. The conventional delivery vectors, such as lentivirus (LV) and adeno-associated virus (AAV) systems, offer efficient patterns to transport gene editing components into cells [8]. However, these viral vectors face some limitations. The limited packaging capability of AAV vectors, which can accommodate approximately 5 kb of DNA, is a critical factor to consider in gene delivery applications [9]. This constraint significantly narrows the utility of AAVs for delivering gene editing tools, particularly since the size of most BEs and prime editors (PEs) that incorporate the standard SpCas9 exceeds the capacity of a single AAV vector. In addition, the potential for prolonged exposure to active CRISPR components, and risks of unwanted genomic integration, which could lead to cellular toxicity and oncogenesis [10].

Given these challenges, there is a pressing need to explore and define non-viral delivery platforms. For example, lipid nanoparticles (LNPs) serve as a non-viral delivery system for gene editing tools. LNPs offer advantages such as biocompatibility, ease of production, and reduced immunogenicity, making them effective for delivering mRNA-based therapeutics, as demonstrated

in mRNA vaccines [11]. Virus-like particles (VLPs) have emerged as another promising non-viral delivery platform. VLPs are defined as non-pathogenic conglomerates of viral proteins designed to encapsulate and transport specific cargo such as mRNAs, proteins, or ribonucleoprotein complexes (RNPs) potentially replacing viral genetic content [12]. These structures originate from pre-existing viral frameworks and harness the inherent viral characteristics conducive to effective intracellular transport. VLPs can efficiently package gene editing components [13–15]. Recent research has coalesced the Cas9 and the retroviral gag to create retrovirus-like particles (RVLPs), such as  $\gamma$ -retrovirus murine leukemia virus (MLV) (gRVLPs and “enhanced” gRVLPs), and various lentivirus-like particles (LVLPs) and its variants [16]. Galla et al. engineer MLV-derived particles encapsulating CRISPR/Cas9 RNA via all-in-one pattern for precise gene knockout applications. However, most VLP systems for delivering gene editing tools rely on HIV-Gag and Pol proteins. For example, Philippe et al. designed the “Nanoblades” VLP incorporating HIV-Gag and Pol proteins. By fusing Cas9 to HIV-Gag and leveraging the transcriptase and integrase activities of Pol, the system achieves efficient encapsulation of Cas9 ribonucleoproteins (RNPs), enabling high editing efficiencies in primary cells and animal models [17]. However, the reverse transcriptase and integrase functions of Pol pose risks of genomic integration and tumorigenesis. Integrase can randomly insert foreign genes into the host genome, potentially activating oncogenes or disrupting tumor suppressor genes, leading to abnormal cell proliferation. For instance, in treating X-linked severe combined immunodeficiency (SCID-X1) with retroviral vectors, random integration of the vector could activate the oncogene LMO2, which has been confirmed to exert predominant role in acute lymphoblastic leukemia [18].

To mitigate these risks, researchers have developed integration-deficient lentiviral vectors (IDLVs) by mutating integrase sequences to reduce integration risks [19]. However, residual activity of the mutated integrase and off-target integration events through NHEJ or circular DNA recombination pathways remain potential hazards [20, 21]. Such uncontrolled integration could result in genomic instability or tumorigenesis. Moreover, reverse transcriptase activity may trigger immunogenic epitopes, causing adverse immune responses [22].

Consequently, retaining HIV-Pol protein in LVLP for gene editing tool delivery introduces significant genomic integration risks.

To address the limitations of existing delivery systems, this study introduces a safer and more efficient lentivirus-like particle (LVLP) platform for delivering gene editing tools. This system employs a “Gag-Only” strategy, leveraging the self-assembly properties of the HIV-Gag protein while omitting the Pol protein, thereby eliminating risks associated with reverse transcriptase and integrase activities. Multiple mRNA packaging strategies were explored, including the MS2–MS2 coat protein (MCP) interaction, PP7–PP7 binding protein interaction, and psi–Gag interactions, to encapsulate the PAM-less base editor CE-8e–SpRY alongside sgRNA targeting the PD1 translation initiation codon (ATG). The packaging efficiencies of these strategies were systematically evaluated to identify the optimal approach. To assess the base editing performance, a stable PD1-expressing 293T reporter cell line was developed. Incorporating the hepatitis delta virus ribozyme (HDVrz) into the psi packaging signal element further enhanced sgRNA stability, improving the LVLP functionality. Finally, the editing efficiency of the LVLP system was tested across multiple gene targets and cell types, demonstrating its versatility and potential for broader applications.

By optimizing the LVLP platform, this study addresses critical safety concerns while enhancing the efficacy of gene editing tool delivery. These results establish a foundation for developing advanced, robust delivery platforms and expanding the therapeutic potential of gene editing technologies.

## Materials and methods

### Cell culture

Lenti-X 293 T cell line (Taraka) and HEK 293 T cell line (ATCC), and PD1-293 T cell line were cultured in the DMEM (Gibco) with 10% FBS, and 1% penicillin streptomycin (Gibco). Human Jurkat cell line was maintained at the RPMI 1640 medium (Gibco). All cells were maintained at 37°C with 5% CO<sub>2</sub>.

### LVLP generation

LVLPs were produced by the transient transfection of Lenti-X 293 T cells at T75 flasks. Cells were plated in the T75 flasks at a density of  $1.5 \times 10^7$  cells per flask 20–24 h before LipoMax transfection. The detailed plasmid usage is listed in Supplementary materials. The cells were first washed by PBS once again to remove the remaining plasmid and then were replaced by fresh medium 16–18 h after plasmid transfection. We collected the supernatants at 48 and 72 h timepoints post transfection and

centrifuged 4000 g at 4 °C for 30 min to remove cell debris or passed a 0.45 μm filter. The clarified LVLP-containing supernatant were mixed with Lenti-X Concentrator (Taraka) and incubation for overnight at 4 °C according to the manufacture’s’ protocol. After incubation, the LVLP pellet were resuspended by 1%–1% volume cold PBS after centrifugation at 1500 g at 4 °C for 50 min. The purified LVLP was then frozen at – 80 °C in aliquots until use.

### Plasmid transfection

Plasmids were extracted using EndoFree Plasmid Midi Kit (CW2105, Cwbio) and tested the concentration by Nanodrop. HEK293T cells were seeded for transfection at 24-well plates at a 50–70% of density. After 20–24 h, cells were transfected with 2 μl LipoMax and 0.8 μg plasmid DNA. Unless stated otherwise, 0.53 μg CE-8E-SPRY and 0.27 μg sgRNA plasmid were incubated with Opti-MEM transfected into cells for each well after incubation for 25 min at room temperature. The medium was refreshed after 4–6 h. After 48–72 h of transfection, 20,000 cells (eGFP-positive) were harvested by fluorescence-activated cell sorting (FACS) in BD Aria II and then for following base editing analysis.

### LVLP transfection

20000 HEK293T cells, or PD1-293T reporter cells, were plated at 24 well plates before transfection. Then 20 ng LVLP (determined by ELISA) was added into target sample. When performing luciferase assay, 2000 PD1-293T reporter cells were plated at the 96-well plate and 5 ng LVLP (determined by ELISA) was used for transfection. After 24 h, cell medium was refreshed and we collected the cell sample 48–72 h later. The cells were lysed for the following base editing analysis or western blot analysis.

### ELISA

The concentration of LVLPs produced in current study was quantified using the p24 ELISA kit (JL19101, JnlIn). We diluted LVLP samples ranging from 1:100 to 1:1000 within the universal dilution buffer from the ELISA kit and then performed ELISA assay according to manufactures’ instruction. We established the quantitation curve using a series of standard p24 reagent. 100 μL of either the sample or the standard reagent of varying concentrations were added into the designated wells. Then of biotinylated antibody working solution was added into the well and incubation at 37 °C for 1 h. Next, liquid was discarded and 300 μL working wash solution was used to wash for three times. Then 100 μL of enzyme conjugate working solution was added into each well and incubation for 30 min. After washing for 5

times, 90  $\mu$ L of substrate solution (TMB) was added into each well and incubation for 15 min. Finally, 50  $\mu$ L stop solution was directly added to each well and we tested the OD value of each sample at a wavelength of 450 nm using the SpectraMax iD3 (Molecular Devices). The p24 content of the LVLPs was determined by comparing it to a series of dilutions of p24 standard curve.

#### **LVLP transfection**

RNA of concentrated LVLPs was extracted using the DOF-9648 Purification Instrument (GenMagBio, China) via RNA isolation kit (GMB-V-F4, GenMagBio). Alternatively, RNA isolation was performed directly from 140  $\mu$ L of particle-containing supernatant using the QIAamp Viral RNA Mini Kit (QIAGEN). Trizol reagent was used to isolate RNA from cells.

#### **In vitro transcript assay**

To exactly measure the mRNA content of LVLP, we firstly generated the CE-8e-SPRY mRNA by in vitro transcription assay (IVT) via using HyperScribe™ All in One mRNA Synthesis Kit Plus 1. Briefly, we generated the CE-8e-SPRY DNA templates by PCR and remove the original plasmid via gel extraction assay. Then transcription reaction was performed and DNase I was used remove original DNA template. Next, we performed the tailing reaction via E-PAP Buffer based on the manufacture's protocol. Finally, phenol–chloroform extraction and ethanol precipitation strategy were used to purify the RNA transcription products. The RNA concentration was measured using a UV spectrophotometry at 260 nm. We designed the primers and probes target CE-8e-SpRY and verified it at plasmid level. Then we conducted RT-qPCR assay by taking the CE-8e-SPRY mRNA with different concentration as the template through the One Step PrimeScript™ RT-PCR Kit (Perfect Real Time) (RR064A, Taraka). The mRNA copy number was calculated by the following formula: number of RNA copies = amount (ng)  $\times$   $6.022 \times 10^{23}$  / (length (bp)  $\times$   $1 \times 10^9 \times 330$ ). The standard copy number curve of CE-8e-SpRY was created and could be used to quantify the mRNA content within LVLP.

#### **Quantification of sgRNA abundance by ddPCR**

We first certified the efficiency of the primers and probes targeting sgRNA at the plasmid level. Total RNA within LVLPs was acquired using DOF-9648 Purification Instrument (GenMagBio, China) via RNA isolation kit (GMB-V-F4, GenMagBio). DNase I (Beyotime) treatment was applied to eliminate any remaining plasmid DNA. Quantitative droplet digital PCR (ddPCR) was carried out on Sniper DQ24 Digital PCR system, employing One Step RT- dPCR Master Mix for Probes (Sniper).

#### **Western blot**

For viral proteins from lentivirus and LVLPs, 100 ng of purified lentivirus or LVLPs (determined by p24 ELISA) were lysed in loading buffer and then boiled for 3–5 min. Proteins derived from cells was isolated via RIPA buffer according to previous protocol. The proteins were separated on SDS-PAGE gels and transferred into a PVDF membrane. The antibodies used included PD1 (NAT105, ab52587, Abcam, 1:50),  $\beta$ -actin antibody for positive control (AA128, Beyotime, 1:1000). After washing the membrane, marching secondary antibodies was mixed with the membrane. Chemiluminescent reagents (Pierce) were used to visualize protein signals.

#### **Base editing efficiency analysis**

For cell samples with FACS, 20000 cells were usually harvested and treated with 20 cell lysis buffers (50 mM KCl, 1.5 mM MgCl<sub>2</sub>, 10 mM Tris pH 8.0, 0.5% Nonidet P-40, 0.5% Tween 20, 100  $\mu$ g/mL protease K) under the following conditions: 65 °C for 30 min, 98 °C for 3 min. For cells transfected with LVLPs, lysis product was used the DNA template for PCR. Primers were listed in supplementary materials. The PCR products were used for Sanger sequencing and the A-to-G base-editing efficiency was evaluated by EditR online tool.

#### **Luciferase assay**

The Bright-Lite Luciferase Assay System (DD1204, Vazyme) is an ultra-sensitive, stable, and homogeneous reagent designed for the detection of firefly luciferase reporter genes. The assay system contains highly purified luciferin and optimized reaction reagents, which enhance reaction stability, improve environmental tolerance, and reduce odor. By directly adding the mixed bright-lite assay reagent to cell cultures, cells are lysed, releasing luciferase, which produces a stable light signal. 2000 PD1-293T reporter cells were plated at 96-well plate. After 24 h, 5 ng LVLP (determined by ELISA) was used to transfect the cells and cell culture supernatant was replaced by fresh medium after 24 h. After transfection 48–72 h, cell was mixed with an equal volume of room temperature-equilibrated bright-lite assay reagent buffer. The mixture was incubated for at least 2 min to ensure complete cell lysis. Then, we tested the firefly luciferase value of each sample via GloMax (Promega).

#### **Transmission electron microscope imaging**

For the process of negative staining, LVLP supernatant was concentrated by Lenti-X concentrator (Taraka). Carbon grids were then immersed in 20  $\mu$ L of the LVLP sample, after which the particles were stained with phosphotungstic

acid. The samples were subsequently dried and examined using a FEI Tecnai 12 electron microscope (CDC, China).

### Mendelian randomization analysis

MR analysis was used to investigate the causal relationships between genetic variants and methylation sites of PD1 (ENSG00000188389), B2M (ENSG00000166710), CIITA (ENSG00000179583), TRAC (ENSG00000277734), and TIGIT (ENSG00000181847) genes and various cancers. We used both expression quantitative trait loci (eQTL) and methylation data as exposures by <https://gwas.mrcieu.ac.uk/datasets/> website. The outcome data were also extracted from genome-wide association studies (GWAS) datasets for multiple cancers. Instrumental variables (IVs) for the exposures were selected based on a genome-wide significance threshold ( $p$ -value <  $1e-06$ ). Exposure data were harmonized with the outcome data to align the effect alleles. SNPs that were palindromic with intermediate allele frequencies were excluded to avoid ambiguity. Further, SNPs were filtered based on their  $F$ -statistics to ensure they were strong instruments ( $F > 10$ ). The heterogeneity and pleiotropy between SNPs were evaluated by Cochran's  $Q$  test and the MR-Egger intercept test. The leave-one-out analysis confirmed that the results were not driven by any single SNP. For MR sensitivity analysis, pleiotropy residual sum and outlier (MR-PRESSO) was used to reduce bias caused by correlated horizontal pleiotropy by using TwosampleMR package. Bayesian colocalization analysis was used to assess the probability that two traits share the same causal variant, using the coloc package with default parameters (<https://github.com/chr1swallace/coloc>) according to previous study [23]. We defined the threshold for colocalization evidence as  $PP.H4.abf > 80\%$ . Visualization was performed using the locuscompare package.

### Statistical analysis

The data are expressed as mean  $\pm$  standard deviation (SD). The unpaired  $t$ -test and ANOVA were used to determine significant differences between two groups and more than two groups, respectively. All statistical analyses were conducted using GraphPad Prism v8. Significant  $P$ -values (unpaired  $t$ -test and ANOVA) are marked by  $*P < 0.05$ ,  $**P < 0.01$ ,  $***P < 0.005$ . All data are presented as mean  $\pm$  SD of triplicates. MR analysis was conducted in R project (4.4.1).

## Results

### Feasibility of constructing LVLPs using the Gag-Only strategy

We first evaluated the feasibility of constructing LVLPs using the HIV-Gag protein without the Pol protein, referred to as the "Gag-Only" strategy. To achieve this,

we introduced the chemically inducible dimerization (CID), FKBP-FRB (FK506-binding protein–FKBP-rapamycin binding protein) interaction system [24]. To test this system, we constructed an HIV-Gag vector retaining only the MA/CA/NC/p6 domains, with the FKBP domain fused to the N-terminus of HIV-Gag and the FRB domain fused to the N-terminus of luciferase (Fig. 1A). To generate LVLPs, we co-transfected plasmids encoding FKBP-HIV-Gag, FRB-luciferase, and VSV-G into cells (Fig. 1B). Then we detected the luciferase activity within LVLP. Compared with control, LVLPs showed significantly higher luciferase activity (Fig. 1C), demonstrating that the Gag-Only strategy effectively generated LVLPs capable of encapsulating luciferase protein. We transfected luciferase-containing LVLPs into 293 T cells and observed the presence of intracellular luciferase signal based on elevated luciferase activity in recipient cells (Fig. 1D). Transmission electron microscopy (TEM) revealed that LVLPs formed using the Gag-Only strategy exhibited a spherical morphology of 100–130 nm, consistent with the size of HIV particles (Fig. 1E). We also observed the presence of Gag protein in the LVLPs (Fig. 1F). Collectively, these results validated the feasibility of the Gag-Only strategy for producing LVLPs capable of encapsulating and delivering target proteins.

### Development of LVLP system for encapsulating CE-8e-SpRY mRNA

Building on the CE-8e-SpRY base editor, which exhibits minimal PAM constraints [25], we explored and validated multiple mRNA packaging strategies for LVLP. To elucidate the mechanisms underlying mRNA encapsulation, we employed RNA–protein interactions such as MS2-MCP (MS2 coat protein), PP7-PP7 BP (PP7 binding protein), and psi-HIV-Gag. Several packaging schemes were designed to incorporate these interactions into the LVLP system (Fig. 2A). For the psi-Gag system, the psi sequence was cloned into CE-8e-SpRY. In the MS2-MCP system, the MS2 sequence was fused to the C-terminus of CE-8e-SpRY, and MCP was fused to the C-terminus of HIV-Gag. Similarly, for the PP7-PP7 BP system, the PP7 sequence was fused to CE-8e-SpRY, and PP7 BP was fused to HIV-Gag. PD1 emerges as pivotal target for cancer therapy and PD1 inhibitors restore T-cell antitumor activity. The translation start codon (ATG) of PD1 is a critical target for RNA editing and regulation. Given the editing window of CE-8e-SpRY (8 bp), we designed two sgRNAs targeting the PD1 ATG codon: one for the A-site and the other for the reverse T-site, referred to as sgRNA and FX-sgRNA, respectively (Fig. 2B). These sgRNAs were cloned into the pGL3-U6-sgRNA-PGK-EGFP vector. We tested the base

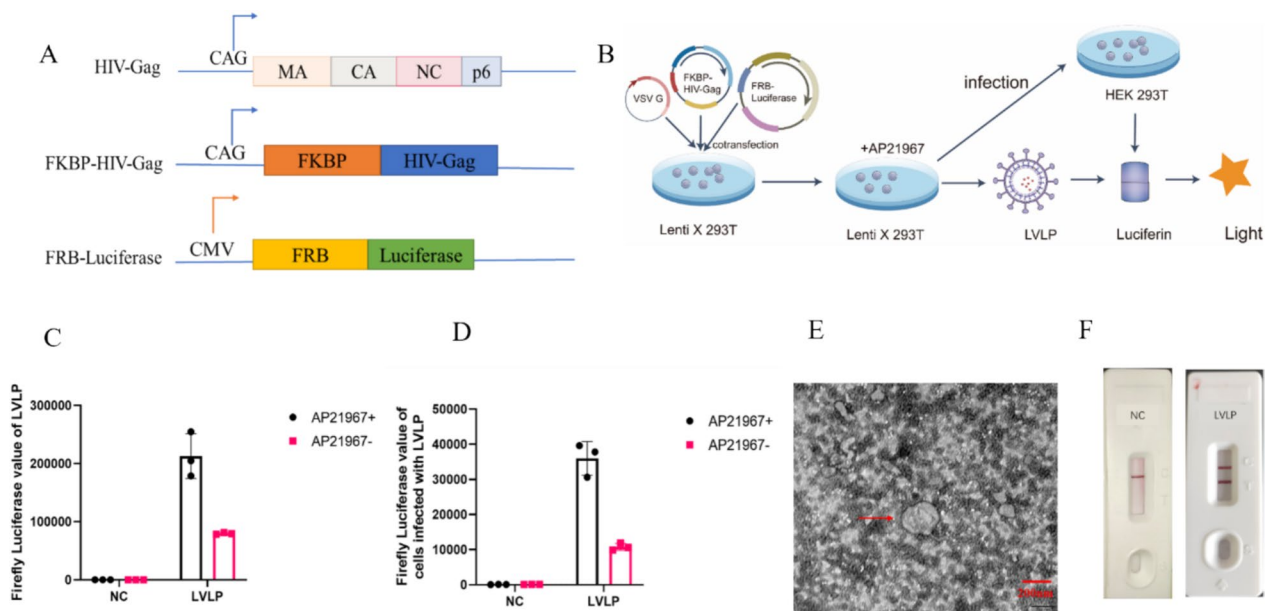


**Fig. 1** Feasibility validation of constructing LVLPs with the Gag-Only strategy. **A** Schematic diagram of HIV-Gag/FKBP-HIV-Gag/FRB-Luciferase plasmid. **B** Schematic diagram of luciferase-containing LVLV prepared based on FKBP-FRB and infected with 293T cells (AP21967 stands for rapamycin analog). **C** Luciferase activity of particles within LVLV (where NC group is the supernatant of cell culture without transfected plasmid, and AP21967 ± indicates that AP21967 was added or not during LVLV generation,  $n=3$ ). **D** Luciferase activity in 293T cells transfected with LVLV after 48h ( $n=3$ ). **E** Transmission electron microscopy of luciferase-LVLV (200 nm). **F** Detection results of LVLV p24 using colloidal gold rapid test card (line C indicates the control line, and line T indicates the detection of HIV-Gag protein in LVLV, where the NC group is the cell culture supernatant without transfected plasmid)

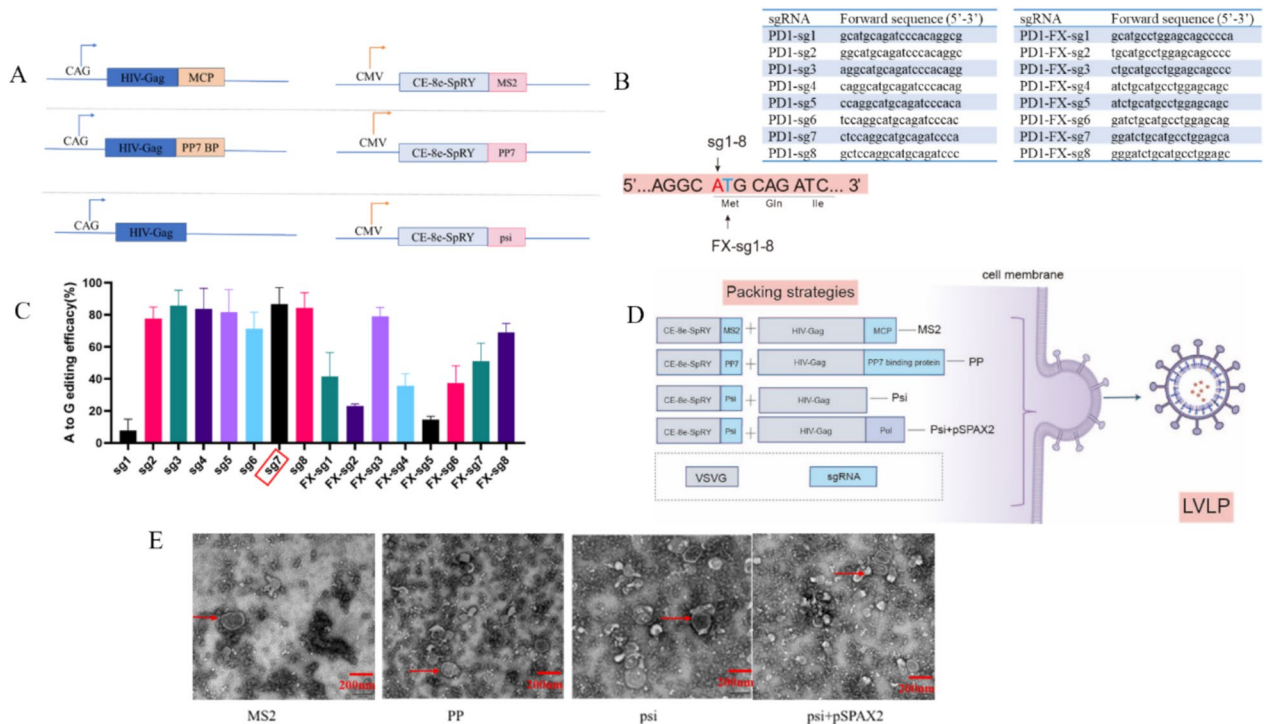


**Fig. 2** Establishment of LVLV system for encapsulating CE-8e-SpRY. **A** Plasmid design of HIV-Gag-MCP/HIV-Gag-PP7 BP/HIV-Gag, CE-8e-SpRY-MS2/CE-8e-SpRY-PP7/CE-8e-SpRY-psi. **B** Schematic design of mRNA generation by MS2-MCP, PP7-PP binding protein, psi-GAG, Psi + pSPAX2 via LVLV. **C** Illustration of sgRNA and FX-sgRNA design targeting the A site of PD1 CDS. **D** A-to-G editing efficiency of 8 sgRNAs and 8 FX-sgRNAs. **E** Transmission electron microscopy of several LVLVs (200 nm)

editing efficiency of sgRNA in HEK293T cells. Results revealed that PD1-sg7 exhibited the highest editing activity (Fig. 2C). As a result, PD1-sg7 was subsequently used to produce LVLPs (Fig. 2D). We used the pSPAX2 plasmid, a second-generation lentiviral packaging vector containing both HIV-Gag and Pol proteins, as a control. We further analyzed the morphology of LVLPs using TEM. The results revealed that several LVLPs exhibited characteristic spherical structures with sizes consistent with HIV particles (Fig. 2E). These observations validate the feasibility of constructing LVLPs encapsulating mRNA using only the HIV-Gag protein.

**Psi-LVLP indicated high mRNA packing efficiency**

The p24 protein, encoded by the HIV-Gag gene, is a core component of the HIV capsid and plays a critical role in forming the structural backbone of VLP. During LVLP assembly, Gag proteins self-assemble to form the particle core, making p24 expression levels a reliable indicator of LVLP production efficiency. To quantify LVLP production, we measured p24 levels using ELISA assay. A standard curve was generated with known concentrations of p24 antigen to ensure p24 levels in

LVLP (Fig. 3A). We analyzed p24 concentrations in several LVLP preparations and found that the Gag-Only packaging strategies did not exhibit significant reductions in production efficiency compared to the control group (psi + pSPAX2, Gag + HIV-Pol) (Fig. 3B). Among the packaging strategies tested, the psi-LVLP scheme demonstrated the highest level of HIV-Gag expression. These results validated the feasibility of using the Gag-Only strategy for LVLP construction and highlighted the psi-LVLP strategy as the most efficient approach for LVLP production. Then CE-8e-SpRY mRNA was generated by IVT assay for the following quantitative assay (Fig. 3C). We developed a system to determine the CE-8e-SpRY mRNA copy number to exactly assess the cargo RNA contents in the LVLPs (Fig. 3D). We conducted RT-PCR reaction by taking mRNA with different concentrations as template. The copy number was acquired of matching mRNA concentration according to the formula:  $\text{number of RNA copies} = \text{amount}(\text{ng}) \times 6.022 \times 10^{23} / (\text{length}(\text{bp}) \times 1 \times 10^9 \times 330)$ . We established the standard curve of CE-8e-SpRY mRNA copy number (Fig. 3E). Furthermore, we extracted the RNA from the LVLPs and treated with DNase I to

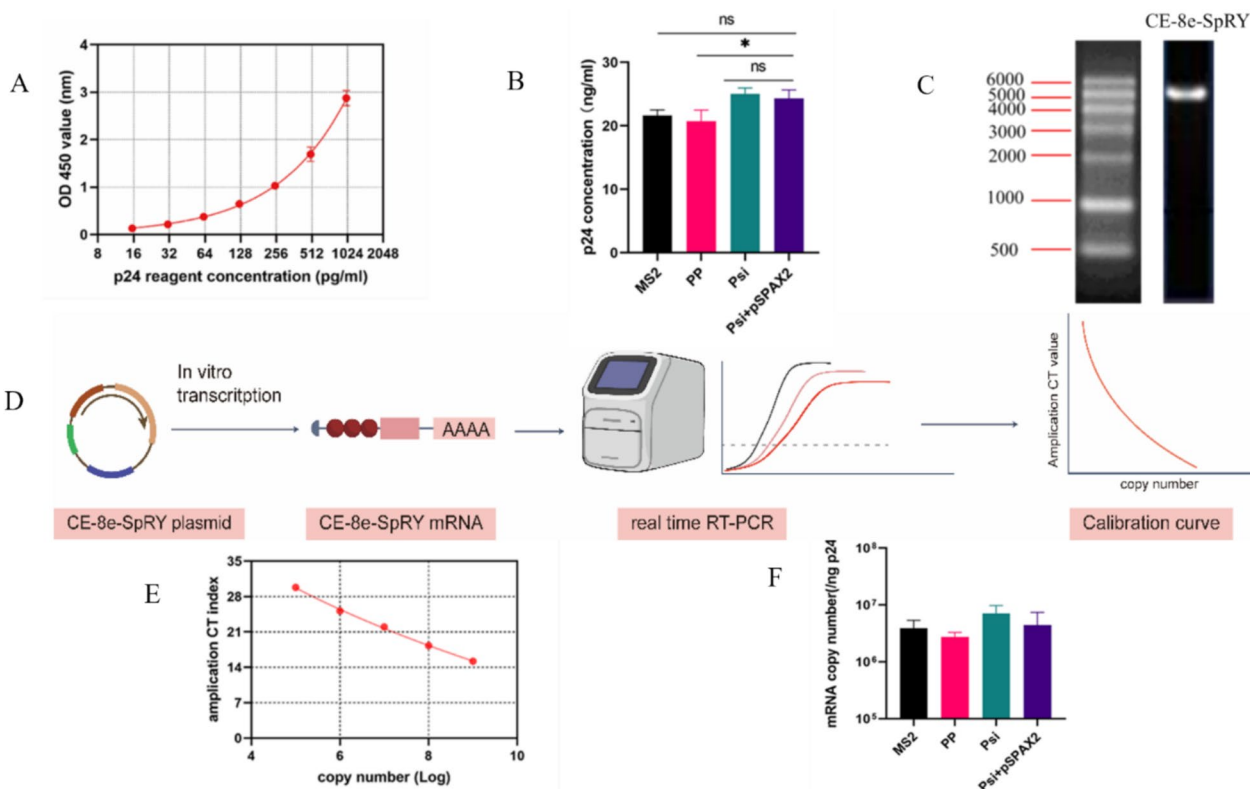


**Fig.3** Packing efficiency of several LVLPs. **A** The standard quantitation curve of p24 reagent determined by ELISA. **B** p24 concentration of LVLPs generated by several packing strategies (corresponding to 2D). **C** Electropherogram of CE-8e-SpRY mRNA obtained from in vitro transcription. **D** Workflow of CE-8e-SpRY mRNA quantification assay. **E** CE-8e-SpRY mRNA copy number-Ct standard curve (n=3). **F** mRNA copy number contained in different LVLPs (each 1ng p24, n=3)

eliminate the influence of any remaining plasmid DNA. Copy number analysis showed psi-LVLP contained the highest levels of mRNA compared to the MS2 and PP7-based strategies (Fig. 3F). This may be attributed to its more efficient RNA transcription or improved RNA stability.

**Psi-LVLP displayed high gene editing efficiency**

To evaluate the component efficiency of LVLP-containing sgRNA that aim to disrupt PD1 expression, we developed a 293T cell line that stably expressed PD1 protein by using lentivirus packaging system (Fig. 4A). Specially speaking, we created the dual-reporter system that contained luciferase and RFP elements. Luciferase reporter gene was cloned at the 3' terminal of PD1 CDS region, whose expression could be evaluated by assessing luciferase activity. RFP was cloned at the 3' terminal of luciferase and used to repress the integration of PD1 gene into the genome (Fig. 4B). After puro screening, we verified the high firefly luciferase activity of PD1-293T cell line (Fig. 4C). qRT-PCR assay indicated the PD1 expression in PD1-293T cell line

(Fig. 4D). Image analysis showed the presence of RFP in PD1-293T cell line (Fig. 4E). Also, WB assay certificated the presence of PD1-luciferase fusion protein in PD1-293T cell line (Fig. 4F). These data showed that we have developed a PD1-293T reporter cell line that firmly expressed PD1 protein, which served as an effective platform for LVLP efficiency evaluation. To evaluate the editing efficiency of LVLPs in PD1, the particles were transfected into PD1-293T cells, and changes in PD1 expression levels were assessed using a luciferase detection system. The results demonstrated a reduction in luciferase activity in cells infected with LVLPs, with the psi-LVLP strategy exhibiting the most significant inhibitory effect (Fig. 4G), confirming the gene editing efficacy of LVLPs. Next, we compared the base editing efficiency of different LVLP packaging strategies. Without FACS sorting, psi-LVLPs achieved the highest base editing efficiency, approximately 15% (Fig. 4H). These findings indicate that, compared to other strategies, the psi-LVLP enables the encapsulation of higher mRNA levels within particles, resulting in efficient gene editing functionality.

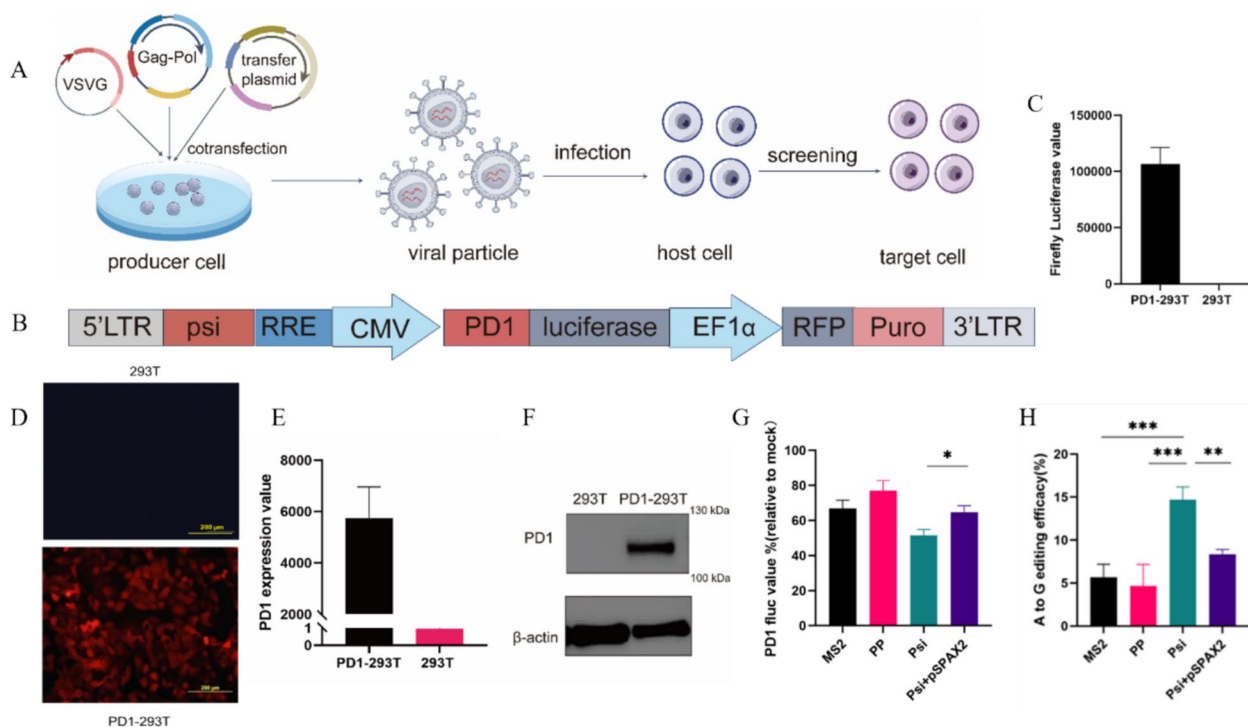


**Fig. 4** Gene editing efficiency analysis of several LVLPs. **A** Schematic diagram of the PD1-293T cell line construction process using lentivirus packing technology. **B** Schematic diagram of pLVX-PD1-luciferase-RFP-puro expression vector (LTR: long terminal repeat; RRE: Rev response element; RFP: red fluorescent protein). **C** Fluorescence values of 293T and PD1-293T cell lines ( $n=3$ ). **D** RFP images of PD1-293T and 293T cells (200  $\mu$ m). **E** PD1 mRNA expression levels of 293T cells and PD1-293T cells (mRNA expression values were calculated as  $2^{-\Delta\Delta Ct}$ ,  $n=3$ ). **F** PD1 protein expression levels in 293T and PD1-293T cells. **G** Luciferase activity of PD1-293T cells treated with different LVLPs (relative to the same number of uninfected LVLPs with PD1-293T cells,  $n=3$ , \* $P < 0.05$ ). **H** Base editing efficiency of LVLP in 293T cells (20ng LVLP per 20,000 cells,  $n=3$ , \*\* $P < 0.01$ , \*\*\* $P < 0.005$ )

### Optimizing the component stoichiometry of LVLP enhanced gene editing efficiency

To enhance the production of LVLPs while maintaining their effectiveness, we investigated the influence of plasmid stoichiometry on LVLP synthesis by fine-tuning the proportions of transfected plasmid DNA (Supplementary Table 1). This adjustment aims to optimize the balance, potentially leading to higher yields without compromising functional integrity (Fig. 5A). In our study, we examined 12 different ratios of the packaging plasmids (Gag and CE-8e-SpRY) during the production process. We observed an increase in p24 yield with a higher amount of the Gag/CE-8e-SpRY-psi combination (Fig. 5B), and high base editor mRNA contents (Fig. 5C) even in different stoichiometry contexts, indicating that psi positively impacted LVLP production. We also examined the gene disruption by luciferase assay in the transgenic PD1-293T reporter cell lines (Fig. 5D). In consistent with this, psi-LVLP displayed the highest A-to-G editing of PD1 in transgenic 293T cells without FACS (Fig. 5E). We selected the V4 ratio as it retained full activity with only a negligible drop in yield.

### HDVrz-psi-sgRNA modified LVLP displayed high base editing efficiency

Achieving effective base editing through LVLP relies heavily on the successful expression and precise processing of sgRNAs. Considering the powerful packing efficiency of psi scheme in LVLP generation, we hypothesized that the introduction of packing signal would tempt the cargo mRNA into the LVLP particles. We added the psi agent in the sgRNA scaffold. Previous study has found that HDVrz is incorporated into the CRISPR-Cas9 system to ensure precise processing of gRNAs [26]. Its self-cleaving activity generates accurate 5' and 3' RNA ends, which are crucial for the stability and functionality of gRNAs [27]. As a result, to maximize the recognition character and the access to the LVLP of sgRNA backbone, we placed the HDVrz-psi element at the C-terminus of sgRNA scaffold while HDVrz served as a cleavable linker to promote the sgRNA release after entering into LVLP (Fig. 6A). Furthermore, we determined the influence of HDVrz-psi on base editing activity by transfecting plasmid. Introduction the HDVrz-psi would not eliminate the gene editing ability while retaining the considerable

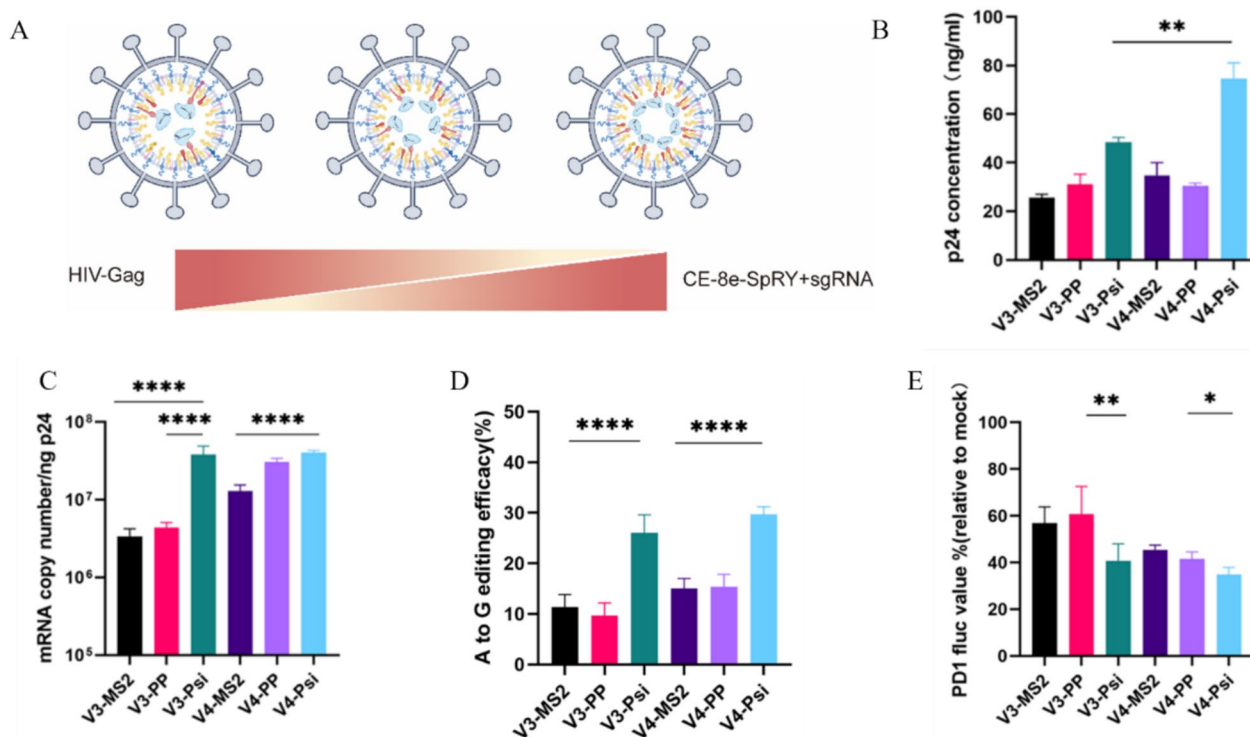


**Fig. 5** Optimizing the component stoichiometry of LVLP increased base editing efficiency. **A** Schematic diagram of LVLP production with different plasmid dosages. **B** The p24 content in several LVLPs with different plasmid ratios ( $n=3$ ,  $**P<0.01$ ). **C** The mRNA copy numbers contained in 1 ng of p24 in LVLP with different plasmid ratios ( $n=3$ ,  $****P<0.0001$ ). **D** Base editing efficiency of several LVLPs in 293T cells with different plasmid ratios (20ng LVLP per 20,000 cells,  $n=3$ ,  $****P<0.0001$ ). **E** Luciferase activity of PD1-293T cells transfected with different LVLPs (relative to the same number of PD1-293T cells uninfected with LVLP,  $n=3$ ,  $*P<0.0001$ )

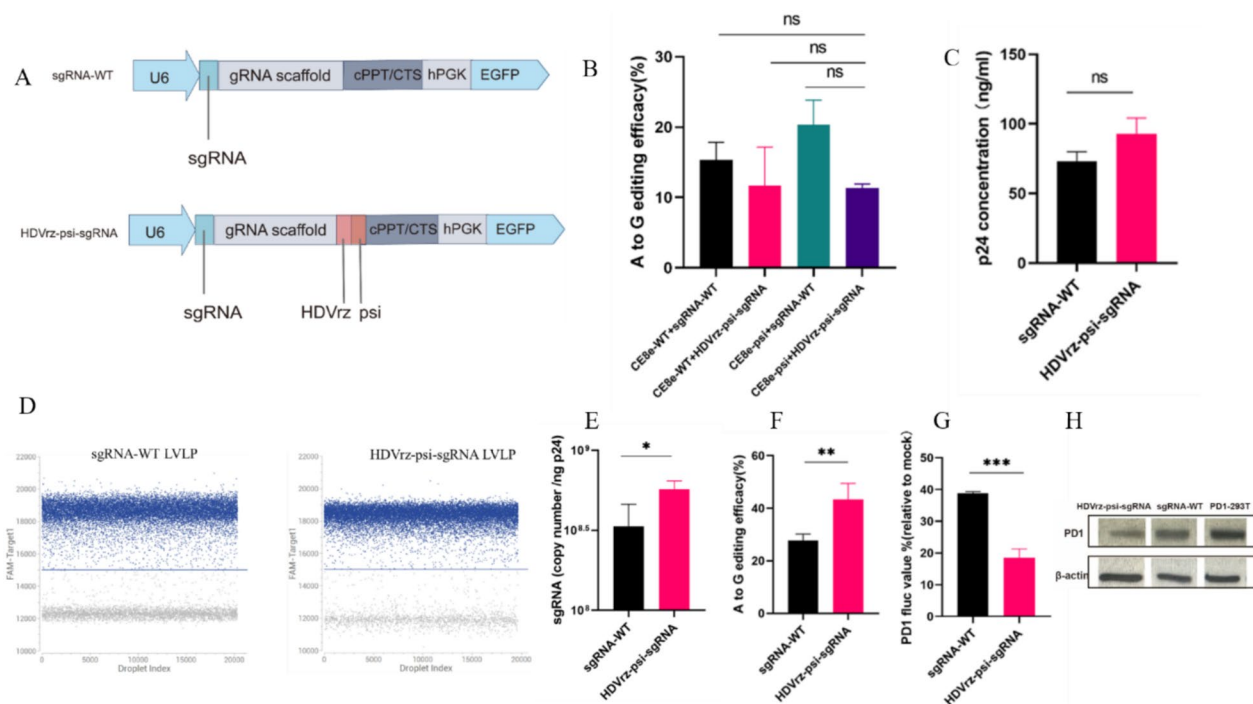


**Fig. 6** HDVrz-psi-sgRNA modified LVLP suggested high base editing efficiency. **A** Schematic design of HDVrz-psi-sgRNA plasmid. **B** Base editing efficiency of different plasmid combinations in 293T cells (CE8e-WT denotes CE-8e-SpRY plasmid, CE8e-psi denotes CE-8e-SpRY-psi plasmid,  $n=3$ , ns denotes no statistical difference). **C** The p24 concentrations of WT-sgRNA and HDVrz-psi-sgRNA LVLP ( $n=3$ , ns indicates no statistical difference). **D** The amplification results of the ddPCR targeting sgRNA. **E** The sgRNA copy numbers of WT-sgRNA LVLP/HDVrz-psi-sgRNA LVLP. ( $*P < 0.05$ ,  $n=3$ ). **F** Editing efficiency of WT-sgRNA /HDVrz-psi-sgRNA LVLP in 293T cells ( $n=3$ ,  $**P < 0.01$ ). **G** Luciferase activity of PD1-293T cells treated with WT-sgRNA and HDVrz-psi-sgRNA LVLP (relative to the same number of PD1-293T cells uninfected with LVLP,  $n=3$ ,  $***P < 0.005$ ). **H** Western blot results of PD1-293T cells treated with WT-sgRNA and HDVrz-psi-sgRNA LVLP

base editing character (Fig. 6B). Next, we used the psi-modified sgRNA to generate LVLP. The introduction of HDVrz-psi did not produce significant effect on the LVLP generation (Fig. 6C). Subsequently, we examined absolute quantification of sgRNA copy numbers in LVLPs using highly specific and sensitive digital PCR (ddPCR) (Fig. 6D). The introduction of HDVrz-psi significantly enhanced the sgRNA copy number in LVLP content (Fig. 6E,  $p < 0.05$ ). This indicates that psi enhances the packaging efficiency of sgRNA in LVLPs and boosts gene editing efficacy. In consistent with this, the HDVrz-psi modified sgRNA LVLP displayed 50% base editing efficacy in 293T cells (Fig. 6F). Interestingly, upon transfection of HDVrz-psi-sgRNA LVLPs into PD1-293T cells, luciferase activity was significantly reduced, suggesting that HDVrz-psi-sgRNA effectively downregulated PD1 expression (Fig. 6G,  $P < 0.005$ ). Western blot analysis further confirmed a marked reduction in PD1 protein levels (Fig. 6H). These findings demonstrate that HDVrz-psi-sgRNA in LVLPs exhibits high gene editing efficiency and effectively suppresses PD1 expression.

### HDVrz-psi-LVLP exhibits high gene editing activity across multiple genes significantly associated with cancer risk

To evaluate the potential of the psi-LVLP system for delivering gene editing tools, we constructed a fluorescently labeled CE-8e-SpRY-psi-EGFP plasmid (Supplementary Fig. 1A) for LVLP production. Subsequently, we used LVLPs encapsulating CE-8e-SpRY-psi-EGFP to infect 293T cells. Flow cytometry analysis revealed that LVLPs efficiently infected 293T cells, achieving an infection rate of approximately 40% (Supplementary Fig. 1B). Our previous results demonstrated that psi-LVLP effectively reduces PD1 protein expression, highlighting its potential significance in cancer immunotherapy. Studies have shown that high expression of B2M (MHC class I molecules) and CIITA (MHC class II molecules) is associated with graft-versus-host disease (GVHD) in CAR-T (chimeric antigen receptor-T cell) therapy, and targeting these genes can enhance the antitumor activity of CAR-T cells [28, 29]. Additionally, reducing TRAC (T-cell receptor  $\alpha$  constant) expression has been shown to improve

CAR-T cell efficacy [30]. TIGIT, as an emerging immune checkpoint, holds great potential as a target for tumor immunotherapy [31]. To further explore the relationship between PD1, B2M, CIITA, TRAC, TIGIT, and cancer risk, we performed Mendelian randomization (MR) analysis to provide deeper insights into the clinical applications of psi-LVLP targeting these genes. We used expression quantitative trait loci (eQTL), which regulate mRNA expression levels, and methylation sites of these genes as exposure factors. Genome-wide association study (GWAS) datasets from over 20 cancer types were used as outcome variables (Supplementary Fig. 1C, D). The results revealed significant associations between certain SNPs of B2M, CIITA, PD1, and TIGIT and specific cancer risks (Supplementary Fig. 2A). Further analysis indicated that methylation sites of PD1, B2M, TIGIT, and CIITA were also significantly correlated with cancer risk (Supplementary Fig. 2B). Additionally, eQTL-GWAS colocalization analysis identified shared significant SNPs of B2M, CIITA, PD, and TIGIT associated with cancer (Supplementary Fig. 2C). Based on these findings, we selected B2M, CIITA, and TIGIT for subsequent research. Building on our previous

editing strategy for PD1, we designed a series of sgRNAs targeting the ATG of B2M, CIITA, and TIGIT to achieve gene knockout-like effect through A-to-G base editing. For each gene, 8 forward sgRNAs and 8 reverse sgRNAs (FX-sgRNAs) were designed, and we examined their base editing efficiencies. The results indicated that B2M-sg4, CIITA-FX-sg8, and TIGIT-FX-sg6 exhibited the highest base editing efficiencies (Fig. 7A). Subsequently, we introduced the HDVrz-psi element into the sgRNAs with the highest editing efficiencies (Fig. 7B). Co-transfection of 293T cells with HDVrz-psi-sgRNA and CE-8e-SpRY-psi demonstrated that the incorporation of HDVrz-psi did not significantly affect base editing activity, as the editing efficiencies remained comparable to those without modification (Fig. 7C). These results confirm that the HDVrz-psi modification does not interfere with sgRNA binding to CE-8e-SpRY. We subsequently used the HDVrz-psi-sgRNAs to produce LVLPs and evaluated their base editing efficiencies. In 293T cells, B2M, CIITA, and TIGIT psi-LVLPs demonstrated base editing efficiencies comparable to those achieved with plasmid transfection (Fig. 7D). Similarly, in Jurkat cells, psi-LVLPs targeting PD1, B2M, CIITA, and TIGIT exhibited base

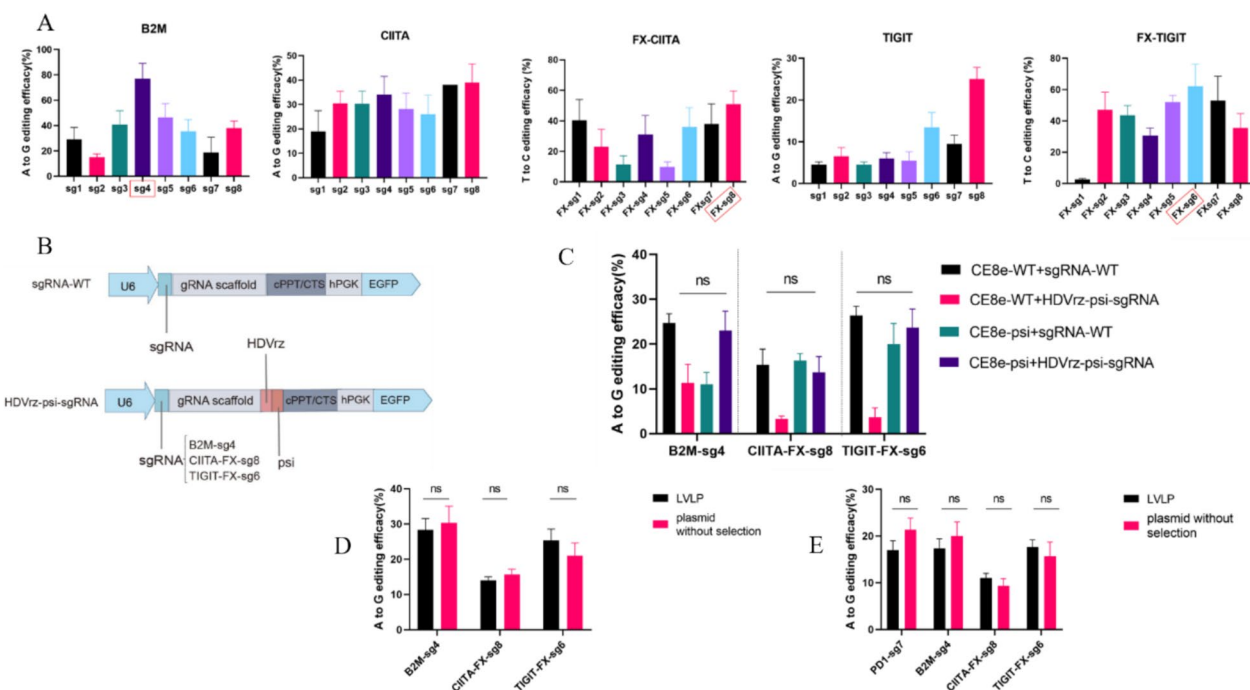


**Fig. 7** HDVrz-psi-LVLP exhibits high gene editing activity across multiple gene loci. **A** Base editing efficiency of B2M/CIITA/TIGIT sgRNA (20,000 cells were FACS and used for PCR sequencing,  $n = 3$ ). **B** Schematic diagram of the design of B2M/CIITA/TIGIT sgRNA-WT and HDVrz-psi-sgRNA plasmids. **C** Base editing efficiency of B2M/CIITA/TIGIT HDVrz-psi-sgRNA and CE-8e-SpRY plasmid (CE8e-WT denotes the CE-8e-SpRY, CE8e-psi denotes the CE-8e-SpRY-psi,  $n = 3$ ). **D** B2M/CIITA/TIGIT HDVrz-psi-sgRNA LVLP base editing efficiency (20 ng LVLP per 20,000 293T cells transfected, plasmid without selection indicated cells were transfected with HDVrz-psi-sgRNA and CE-8e-SpRY-psi plasmid,  $n = 3$ ). **E** PD1/B2M/CIITA/TIGIT HDVrz-psi-sgRNA LVLP editing efficiency (20 ng of LVLP per 20,000 Jurkat cells transfected, plasmid without selection indicated that cells were transfected with HDVrz-psi-sgRNA and CE-8e-SpRY-psi plasmid,  $n = 3$ )

editing efficiencies equivalent to plasmid transfection (Fig. 7E). These findings highlight that targeting these genes with psi-LVLPs can effectively reduce their expression, providing a novel approach to enhancing the antitumor activity of CAR-T therapy.

## Discussion

Non-viral systems such as LNPs have gained prominence for their ability to deliver mRNA with high biocompatibility and minimal immunogenicity, as evidenced by their success in mRNA-based therapeutics. However, their capacity to targeting non-liver system is limited. As noted earlier, intravenously administered LNPs naturally accumulate in the liver due to filtration by sinusoids, uptake by Kupffer cells, and lipoprotein-like interactions with hepatocytes. This biases Cas9 delivery toward the liver [32]. For diseases requiring Cas9 editing in non-liver tissues, LNPs struggle to achieve sufficient delivery and editing efficiency outside the liver without advanced targeting modifications [32]. VLPs have emerged as a promising platform to facilitate the temporary introduction of RNA, or RNP into cells without relying on viral components without the liver tropism compared to LNPs [33, 34]. VLPs circumvent the restriction of universal packaging capacities, minimizing the duration of cellular exposure to genome editing agents [35, 36]. By delivering mRNA or RNPs, VLPs enable rapid degradation of gene-editing tools within cells, minimizing exposure time and potential side effects [37, 38]. Current in vivo applications of LVLPs for gene-editing delivery primarily rely on HIV-Gag and Pol proteins. Retaining integrase and RT in LVLPs can pose several risks due to their roles in viral integration and replication. The integrase (IN) of Pol mediates the random insertion of foreign DNA into the host genome and integration near oncogenes or tumor suppressor genes may lead to cancer [39, 40]. RT plays a crucial role in converting viral RNA into DNA, while this process is accompanied with immunogenic epitopes that could provoke unwanted immune responses [22]. Additionally, HIV exhibits a preference for transcription-active regions, such as enhancers and promoters, further increasing the risk of oncogene activation [41]. Previous studies have demonstrated the potential complications of using integrase-competent systems, including the integration of viral components into the host genome and subsequent genotoxicity [15, 42].

Endeavors to reduce these drawbacks include using IDLV that introduces specific mutations (such as D64, D116, and E152) in the integrase to prevent effective integration of the pro-viral DNA into the host genome, thereby mitigating the risk of insertional mutagenesis [43]. They permit normal DNA synthesis but prevent

integration, resulting in the accumulation of double-stranded DNA within the nucleus. This unintegrated linear DNA can form 1-LTR or 2-LTR circles through long terminal repeat (LTR) recombination or non-homologous end joining (NHEJ). As these circular DNAs lack replication signals, they are gradually diluted during cell division, thereby reducing their integration potential into host DNA [44, 45]. For instance, Nielsen et al. demonstrated the use of an HIV-Gag N-terminal fusion with Cas9 and a D64V HIV-Pol to package Cas9/sgRNA RNPs into VLPs, achieving cell-specific delivery and inducing indel (insertion or deletion) formation [46]. Similarly, Yáñez-Muñoz et al. developed an IDLV with the D64V mutation, reducing HIV integration rates to 1/10,000 of the wild type while maintaining long-term, high-level transgene expression in vivo. However, linear amplification-mediated PCR (LAM-PCR) revealed low-frequency host DNA integration events associated with IDLV [44]. These findings suggest that IDLVs cannot entirely eliminate integrase activity, as residual catalytic activity or abnormal recombination repair mechanisms may still result in genomic insertions, posing uncontrolled integration risks. Consequently, the random integration risks associated with Pol protein-based vectors in gene therapy warrant careful consideration. To address these challenges, we developed a safer LVLP system using the Gag-Only strategy, which eliminates the genomic integration risks associated with HIV-Pol protein. In conventional Gag-Pol systems, this integration is key for stable transgene expression. However, for gene-editing applications where transient delivery is preferred, permanent integration poses an unnecessary safety risk. Our LVLP system leverages a Gag-Only strategy that omits the Pol components, including integrase. This blocked the integration process of foreign DNA at the source. It can be inferred that the Gag-Only system would be near less integration in theory.

In this study, we utilized the interaction between RNA and its specific packaging proteins to establish multiple LVLP mRNA packaging strategies, including MS2-MCP, PP7-PP7 BP, and psi-Gag systems. Among these, the psi-LVLP strategy demonstrated significant advantages in both mRNA packaging and base editing. This can be attributed to psi, a core RNA packaging element derived from HIV, which exhibits high affinity and specificity for the Gag protein, promoting efficient mRNA encapsulation and the self-assembly of virus-like particles. Furthermore, optimizing the Gag/CE-8e-SpRY-psi plasmid ratio significantly improved p24 protein production in LVLPs, which was accompanied by a corresponding increase in mRNA copy numbers. This efficiency likely results from the high affinity between psi and Gag proteins, enabling more RNA to

be packaged into LVLPs. The base editing efficiency of psi-LVLP improved from 15% to approximately 30%. These findings underscore the critical role of psi in enhancing LVLP production and functionality. This aligns with prior research indicating the critical role of selective RNA packaging mechanisms in viral particle assembly [47, 48].

To further enhance LVLP editing efficiency, we introduced HDVrz and psi at the C-terminus of sgRNA. HDVrz is a self-cleaving RNA molecule with multiple stem-loop structures resembling typical RNA secondary structures, enabling precise RNA self-cleavage [49, 50]. Incorporating HDVrz and psi elements at the sgRNA C-terminus ensured the correct 5' and 3' ends for sgRNA. The inclusion of psi also enhanced the binding affinity between sgRNA and Gag proteins, allowing for increased sgRNA encapsulation into LVLPs. To quantify sgRNA content in LVLPs, we employed ddPCR, a highly sensitive and accurate nucleic acid quantification method capable of absolute quantification without being influenced by PCR efficiency. Results showed that HDVrz-psi modified sgRNAs significantly increased sgRNA copy numbers in LVLPs, directly demonstrating the role of psi and HDVrz in improving sgRNA packaging efficiency. In PD1 gene editing, the base editing efficiency increased from 30 to 50%. We also noted that PD1 protein reduced in PD1-293T reporter cells. These results highlight the importance of sgRNA optimization and modification in enhancing LVLP gene editing efficiency.

Currently, most VLPs are designed for delivering CRISPR-Cas9 systems, whereas studies focusing on VLPs for base editing are limited. David et al. developed an engineered VLP by fusing FMLV-Gag with ABE8e, which significantly regulated PCSK9 protein expression in mouse models, demonstrating the potential of base editing for in vivo applications [14]. However, these systems retained the Pol protein, which poses risks of genomic integration. In contrast, our study developed an LVLP system with HIV-Gag protein, eliminating the need for Pol protein and effectively minimizing the risk of genomic integration. Additionally, the encapsulation of PAMless CE-8e-SpRY mRNA in LVLPs overcomes the limitations of traditional base-editing tools that rely on specific PAM sites, expanding the application scope of LVLP-based gene editing. Previous studies have also shown that ABE-induced start codon mutations (e.g., ATG to GTG or ACG) effectively achieve gene knockout [51]. Using a dual-reporter PD1-293T cell line engineered for quantifying PD1 expression through luciferase activity, psi-LVLP demonstrated significant base editing efficiency, effectively reducing PD1 expression. These

results confirm the high gene-editing activity of our LVLP system.

Using MR analysis, we identified significant associations between the gene expression and methylation levels of PD1, B2M, CIITA, and TIGIT genes with cancer risks. Subsequently, we constructed B2M, CIITA, and TIGIT specific psi-LVLPs. In 293T cells, these LVLPs exhibited base editing activity comparable to or higher than plasmid transfection, consistent with previous studies. Mikkelsen et al. demonstrated that VLPs delivering ABE8e achieved gene-editing efficiencies equivalent to plasmid transfection in 293T cells [52]. Furthermore, psi-LVLPs targeting PD1, B2M, CIITA, and TIGIT achieved base editing efficiencies similar to plasmid transfection in Jurkat cells. Compared to DNA transfection, VLPs induced lower cytotoxicity, which is particularly advantageous for sensitive and primary cell types [38]. Additionally, VLPs minimize immune responses triggered by DNA transfection, making it more suitable for therapeutic applications. By regulating gene expression through psi-LVLP base editing, immune cell antitumor activity can be enhanced, providing a promising approach for cancer immunotherapy.

It is important to note that the present study was conceived as a foundational in vitro proof-of-concept for the Gag-Only strategy. While our study successfully establishes the Gag-Only LVLP system for the in vitro delivery of gene-editing tools, several limitations remain that warrant further investigation. First, although our design effectively eliminates the risk of genomic integration associated with HIV-Pol proteins, a comprehensive evaluation of off-target events is critical. The follow-up study involving whole-genome analysis to detect any integration events and off-target sites. This work will provide a more complete safety profile of the LVLP platform. Moving forward, in vivo validation is a key focus of our ongoing research, which will help confirm the efficacy and safety of this approach.

## Conclusion

This study demonstrates the feasibility of a safe and efficient LVLP system for gene-editing tool delivery with Gag-Only strategy, eliminating Pol protein to reduce genomic integration risks. By introducing psi, CE-8e-SpRY mRNA packaging and sgRNA content were significantly enhanced, improving editing efficiency and reducing PD1 protein expression. The psi-LVLP system also exhibited high editing efficiency for multiple cancer-associated genes in 293T and Jurkat cells, highlighting its potential application in tumor immunotherapy and expanding the scope of gene-editing technologies.

## Supplementary Information

The online version contains supplementary material available at <https://doi.org/10.1186/s40001-025-02499-2>.

Supplementary Material 1: Fig.1. Mendelian randomization identified target genes significantly associated with cancer risk. A: CE-8e-SpRY-psi-EGFP plasmid design. B: Flow analysis results of LVLP infected 293T cells carrying CE-8e-SpRY-psi-EGFP mRNA. C: The cancer types that served as the outcome factor in MR study. D: Breast cancer-specific SNPs distribution ring diagram and bar plot within chromosomes. Fig.2. The casual association between B2M/CIITA/TIGIT/PD1 across cancers. A: MR results of significant SNPs of matching genes with cancers. B: MR results of significant methylation sites of B2M, PD1, TIGIT, across cancers. C: The eQTL-GWAS results of significant SNPs of B2M, CIITA, PD1, TIGIT across cancers. Table 1. The generation parameters of the indicated LVLPs configuration. Each value represents the required usage of plasmid per T75 flask. Table 2. sgRNAs of several genes within CE-8e-SpRY editing activity windows. Table 3. PCR primers for PCR and Sanger sequencing. Table 4. PCR primers for qPCR. Table 5. PCR primers for RT-PCR and ddPCR

### Author contributions

JJ,YH,XJ and XM designed the study and performed the assay. L Z helped analyze the base editing. XC helped construct the plasmid. Lisha An assisted in PCR. HW performed FACS. QM helped revise the manuscript. All authors read and approved the final manuscript.

### Funding

This work was funded by grants from the National Key Research and Development Program of China (2016YFC1000307 & 2021YFC2301103).

### Availability of data and materials

No datasets were generated or analysed during the current study.

### Declarations

### Ethics approval and consent to participate

Not applicable.

### Competing interests

The authors declare no competing interests.

### Author details

<sup>1</sup>National Research Institute for Family Planning, Beijing 100081, China. <sup>2</sup>Graduate School, Peking Union Medical College, Chinese Academy of Medical Sciences, Beijing 100005, China. <sup>3</sup>National Human Genetic Resources Center, Beijing 100052, China. <sup>4</sup>National Key Laboratory of Intelligent Tracking and Forecasting for Infectious Diseases, Chinese Center for Disease Control and Prevention, National Institute for Viral Disease Control and Prevention, Beijing 100052, China.

Received: 17 February 2025 Accepted: 24 March 2025

Published online: 04 April 2025

### References

- Wang SW, Gao C, Zheng YM, Yi L, Lu JC, Huang XY, et al. Current applications and future perspective of CRISPR/Cas9 gene editing in cancer. *Mol Cancer*. 2022;21:57. <https://doi.org/10.1186/s12943-022-01518-8>.
- Gupta D, Bhattacharjee O, Mandal D, Sen MK, Dey D, Dasgupta A, et al. CRISPR-Cas9 system: a new-fangled dawn in gene editing. *Life Sci*. 2019;232: 116636. <https://doi.org/10.1016/j.lfs.2019.116636>.
- Cullot G, Boutin J, Toutain J, Prat F, Pennamen P, Rooryck C, et al. CRISPR-Cas9 genome editing induces megabase-scale chromosomal truncations. *Nat Commun*. 2019;10:1136. <https://doi.org/10.1038/s41467-019-09006-2>.
- Murugan K, Suresh SK, Seetharam AS, Severin AJ, Sashital DG. Systematic in vitro specificity profiling reveals nicking defects in natural and engineered CRISPR-Cas9 variants. *Nucl Acid Res*. 2021;49:4037–53. <https://doi.org/10.1093/nar/gkab163>.
- Newby GA, Liu DR. In vivo somatic cell base editing and prime editing. *Mol Ther*. 2021;29:3107–24. <https://doi.org/10.1016/j.ymthe.2021.09.002>.
- Zeng J, Wu Y, Ren C, Bonanno J, Shen AH, Shea D, et al. Therapeutic base editing of human hematopoietic stem cells. *Nat Med*. 2020;26:535–41. <https://doi.org/10.1038/s41591-020-0790-y>.
- Gaudelli NM, Lam DK, Rees HA, Solá-Esteves NM, Barrera LA, Born DA, et al. Directed evolution of adenine base editors with increased activity and therapeutic application. *Nat Biotechnol*. 2020;38:892–900. <https://doi.org/10.1038/s41587-020-0491-6>.
- Ling S, Yang S, Hu X, Yin D, Dai Y, Qian X, et al. Lentiviral delivery of co-packaged Cas9 mRNA and a Vegfa-targeting guide RNA prevents wet age-related macular degeneration in mice. *Nat Biomed Eng*. 2021;5:144–56. <https://doi.org/10.1038/s41551-020-00656-y>.
- Wu J, Zhao W, Zhong L, Han Z, Li B, Ma W, et al. Self-complementary recombinant adeno-associated viral vectors: packaging capacity and the role of rep proteins in vector purity. *Hum Gene Ther*. 2007;18:171–82. <https://doi.org/10.1089/hum.2006.088>.
- Kabadi AM, Ousterout DG, Hilton IB, Gersbach CA. Multiplex CRISPR/Cas9-based genome engineering from a single lentiviral vector. *Nucl Acid Res*. 2014;42: e147. <https://doi.org/10.1093/nar/gku749>.
- Zong Y, Lin Y, Wei T, Cheng Q. Lipid nanoparticle (LNP) enables mRNA delivery for cancer therapy. *Adv Mater*. 2023;35: e2303261. <https://doi.org/10.1002/adma.202303261>.
- Mohsen MO, Bachmann MF. Virus-like particle vaccinology, from bench to bedside. *Cell Mol Immunol*. 2022. <https://doi.org/10.1038/s41423-022-00897-8>.
- Gee P, Lung MSY, Okuzaki Y, Sasakawa N, Iguchi T, Makita Y, et al. Extracellular nanovesicles for packaging of CRISPR-Cas9 protein and sgRNA to induce therapeutic exon skipping. *Nat Commun*. 2020;11:1334. <https://doi.org/10.1038/s41467-020-14957-y>.
- An M, Raguram A, Du SW, Banskota S, Davis JR, Newby GA, et al. Engineered virus-like particles for transient delivery of prime editor ribonucleoprotein complexes in vivo. *Nat Biotechnol*. 2024. <https://doi.org/10.1038/s41587-023-02078-y>.
- Banskota S, Raguram A, Suh S, Du SW, Davis JR, Choi EH, et al. Engineered virus-like particles for efficient in vivo delivery of therapeutic proteins. *Cell*. 2022. <https://doi.org/10.1016/j.cell.2021.12.021>.
- Hamilton JR, Tsuchida CA, Nguyen DN, Shy BR, McGarrigle ER, Sandoval Espinoza CR, et al. Targeted delivery of CRISPR-Cas9 and transgenes enables complex immune cell engineering. *Cell Rep*. 2021;35: 109207. <https://doi.org/10.1016/j.celrep.2021.109207>.
- Mangeot PE, Risson V, Fusil F, Marnef A, Laurent E, Blin J, et al. Genome editing in primary cells and in vivo using viral-derived Nanoblades loaded with Cas9-sgRNA ribonucleoproteins. *Nat Commun*. 2019;10:45. <https://doi.org/10.1038/s41467-018-07845-z>.
- Hacein-Bey-Abina S, Von Kalle C, Schmidt M, McCormack MP, Wulffraat N, Leboulch P, et al. LMO2-associated clonal T cell proliferation in two patients after gene therapy for SCID-X1. *Science*. 2003;302:415–9.
- Ferrari S, Jacob A, Cesana D, Laugel M, Beretta S, Varesi A, et al. Choice of template delivery mitigates the genotoxic risk and adverse impact of editing in human hematopoietic stem cells. *Cell Stem Cell*. 2022. <https://doi.org/10.1016/j.stem.2022.09.001>.
- Delelis O, Carayon K, Saïb A, Deprez E, Mouscadet J-F. Integrase and integration: biochemical activities of HIV-1 integrase. *Retrovirology*. 2008;5:114. <https://doi.org/10.1186/1742-4690-5-114>.
- Philippe S, Sarkis C, Barkats M, Mammeri H, Ladroue C, Petit C, et al. Lentiviral vectors with a defective integrase allow efficient and sustained transgene expression in vitro and in vivo. *Proc Natl Acad Sci U S A*. 2006;103:17684–9.
- Dong W, Kantor B. Lentiviral vectors for delivery of gene-editing systems based on CRISPR/Cas: current state and perspectives. *Viruses*. 2021. <https://doi.org/10.3390/v13071288>.
- Yarmolinsky J, Bouras E, Constantinescu A, Burrows K, Bull CJ, Vincent EE, et al. Genetically proxied glucose-lowering drug target perturbation and risk of cancer: a Mendelian randomisation analysis. *Diabetologia*. 2023;66:1481–500. <https://doi.org/10.1007/s00125-023-05925-4>.

24. Wu HD, Kikuchi M, Dagliyan O, Aragaki AK, Nakamura H, Dokholyan NV, et al. Rational design and implementation of a chemically inducible heterotrimerization system. *Nat Method*. 2020;17:928–36. <https://doi.org/10.1038/s41592-020-0913-x>.
25. Cao X, Guo J, Huang S, Yu W, Li G, An L, et al. Engineering of near-PAMless adenine base editor with enhanced editing activity and reduced off-target. *Mol Ther Nucl Acid*. 2022;28:732–42. <https://doi.org/10.1016/j.omtn.2022.04.032>.
26. Qiao S, Bai F, Cai P, Zhou YJ, Yao L. An improved CRISPRi system in *Pichia pastoris*. *Synth Syst Biotechnol*. 2023;8:479–85. <https://doi.org/10.1016/j.synbio.2023.06.008>.
27. Kennedy AB, Liang JC, Smolke CD. A versatile cis-blocking and trans-activation strategy for ribozyme characterization. *Nucl Acid Res*. 2013;41:e41. <https://doi.org/10.1093/nar/gks1036>.
28. Wang H, Liu B, Wei J. Beta2-microglobulin(B2M) in cancer immunotherapies: biological function, resistance and remedy. *Cancer Lett*. 2021. <https://doi.org/10.1016/j.canlet.2021.06.008>.
29. Santharam MA, Shukla A, Levesque D, Kufer TA, Boisvert FM, Ramanathan S, et al. NLRC5-CIITA fusion protein as an effective inducer of MHC-I expression and antitumor immunity. *Int J Mol Sci*. 2023. <https://doi.org/10.3390/ijms24087206>.
30. Eyquem J, Mansilla-Soto J, Giavridis T, van der Stegen SJC, Hamieh M, Cunanan KM, et al. Targeting a CAR to the TRAC locus with CRISPR/Cas9 enhances tumour rejection. *Nature*. 2017;543:113–7. <https://doi.org/10.1038/nature21405>.
31. Chu X, Tian W, Wang Z, Zhang J, Zhou R. Co-inhibition of TIGIT and PD-1/PD-L1 in cancer immunotherapy: mechanisms and clinical trials. *Mol Cancer*. 2023;22:93. <https://doi.org/10.1186/s12943-023-01800-3>.
32. Raguram A, Banskota S, Liu DR. Therapeutic in vivo delivery of gene editing agents. *Cell*. 2022;185(15):2806–27. <https://doi.org/10.1016/j.cell.2022.03.045>.
33. Piotrowski-Daspit AS, Glaze PM, Saltzman WM. Debugging the genetic code: non-viral in vivo delivery of therapeutic genome editing technologies. *Curr Opin Biomed Eng*. 2018;7:24–32. <https://doi.org/10.1016/j.cobme.2018.08.002>.
34. Song X, Liu C, Wang N, Huang H, He S, Gong C, et al. Delivery of CRISPR/Cas systems for cancer gene therapy and immunotherapy. *Adv Drug Deliv Rev*. 2021;168:158–80. <https://doi.org/10.1016/j.addr.2020.04.010>.
35. Zhang J, Hu Y, Yang J, Li W, Zhang M, Wang Q, et al. Non-viral, specifically targeted CAR-T cells achieve high safety and efficacy in B-NHL. *Nature*. 2022;609:369–74. <https://doi.org/10.1038/s41586-022-05140-y>.
36. Patil S, Gao Y-G, Lin X, Li Y, Dang K, Tian Y, et al. The development of functional non-viral vectors for gene delivery. *Int J Mol Sci*. 2019. <https://doi.org/10.3390/ijms20215491>.
37. Lyu P, Wang L, Lu B. Virus-like particle mediated CRISPR/Cas9 delivery for efficient and safe genome editing. *Life (Basel)*. 2020. <https://doi.org/10.3390/life10120366>.
38. Montagna C, Petris G, Casini A, Maule G, Franceschini GM, Zanella I, et al. VSV-G-enveloped vesicles for traceless delivery of CRISPR-Cas9. *Mol Ther Nucl Acid*. 2018;12:453–62. <https://doi.org/10.1016/j.omtn.2018.05.010>.
39. Yoder KE, Rabe AJ, Fishel R, Larue RC. Strategies for targeting retroviral integration for safer gene therapy: advances and challenges. *Front Mol Biosci*. 2021;8: 662331. <https://doi.org/10.3389/fmolb.2021.662331>.
40. Wang L, Sarafianos SG, Wang Z. Cutting into the substrate dominance: pharmacophore and structure-based approaches toward inhibiting human immunodeficiency virus reverse transcriptase-associated ribonuclease H. *Acc Chem Res*. 2020;53:218–30. <https://doi.org/10.1021/acs.accounts.9b00450>.
41. Ji H, Jiang Z, Lu P, Ma L, Li C, Pan H, et al. Specific reactivation of latent HIV-1 by dCas9-SunTag-VP64-mediated guide RNA targeting the HIV-1 promoter. *Mol Ther*. 2016;24:508–21. <https://doi.org/10.1038/mt.2016.7>.
42. Crunkhorn S. Enhancing base editor delivery. *Nat Rev Drug Discov*. 2022;21:177. <https://doi.org/10.1038/d41573-022-00021-5>.
43. Wanisch K, Yáñez-Muñoz RJ. Integration-deficient lentiviral vectors: a slow coming of age. *Mol Ther*. 2009;17:1316–32. <https://doi.org/10.1038/mt.2009.122>.
44. Yáñez-Muñoz RJ, Balagán KS, MacNeil A, Howe SJ, Schmidt M, Smith AJ, et al. Effective gene therapy with nonintegrating lentiviral vectors. *Nat Med*. 2006;12:348–53. <https://doi.org/10.1038/nm1365>.
45. Verghese SC, Goloviznina NA, Skinner AM, Lipps HJ, Kurre P. S/MAR sequence confers long-term mitotic stability on non-integrating lentiviral vector episomes without selection. *Nucl Acid Res*. 2014;42: e53. <https://doi.org/10.1093/nar/gku082>.
46. Nielsen IH, Røvsing AB, Janns JH, Thomsen EA, Ruzo A, Bøggild A, et al. Cell-targeted gene modification by delivery of CRISPR-Cas9 ribonucleoprotein complexes in pseudotyped lentivirus-derived nanoparticles. *Mol Ther Nucl Acid*. 2024;35: 102318. <https://doi.org/10.1016/j.omtn.2024.102318>.
47. Olson ED, Musier-Forsyth K. Retroviral Gag protein–RNA interactions: Implications for specific genomic RNA packaging and virion assembly. *Semin Cell Dev Biol*. 2019;86:129–39. <https://doi.org/10.1016/j.semcdb.2018.03.015>.
48. Twarock R, Stockley PG. RNA-mediated virus assembly: mechanisms and consequences for viral evolution and therapy. *Annu Rev Biophys*. 2019;48:495–514. <https://doi.org/10.1146/annurev-biophys-052118-115611>.
49. Gao Z, Herrera-Carrillo E, Berkhout B. Improvement of the CRISPR-Cpf1 system with ribozyme-processed crRNA. *RNA Biol*. 2018;15:1458–67. <https://doi.org/10.1080/15476286.2018.1551703>.
50. Berkhout B, Gao Z, Herrera-Carrillo E. Design and evaluation of guide RNA transcripts with a 3'-terminal HDV ribozyme to enhance CRISPR-based gene inactivation. *Method Mol Biol*. 2021;2167:205–24. [https://doi.org/10.1007/978-1-0716-0716-9\\_12](https://doi.org/10.1007/978-1-0716-0716-9_12).
51. Wang X, Liu Z, Li G, Dang L, Huang S, He L, et al. Efficient gene silencing by adenine base editor-mediated start codon mutation. *Mol Ther*. 2020;28:431–40. <https://doi.org/10.1016/j.jymthe.2019.11.022>.
52. Haldrup J, Andersen S, Labial ARL, Wolff JH, Frandsen FP, Skov TW, et al. Engineered lentivirus-derived nanoparticles (LVNPs) for delivery of CRISPR/Cas ribonucleoprotein complexes supporting base editing, prime editing and in vivo gene modification. *Nucl Acid Res*. 2023;51:10059–74. <https://doi.org/10.1093/nar/gkad676>.

## Publisher's Note

Springer Nature remains neutral with regard to jurisdictional claims in published maps and institutional affiliations.